

Stability Analysis of a Three-Dimensional Rectangular Isotropic Plates With Arbitrary Clamped And Simply Supported Boundary Conditions

Onyeka, F. C.^{1,3}, Okeke, T. E.^{2*}, Nwa-David, C. D.³

¹Department of Civil Engineering, Edo State University Uzairue, Edo State.

²Department of Civil Engineering, University of Nigeria, Nsukka.

³Department of Civil Engineering, Michael Okpara University of Agriculture, Umudike.

Corresponding author: edozie.okeke@unn.edu.ng

Abstract: In this paper, a three-dimensional (3D) plate theory was used to investigate the stability analysis of an isotropic thick rectangular plate that is clamped in its three edges and one simply supported edge (CCCS) under uniaxial compression using polynomial displacement function. Using three dimensional constitutive relations, the total energy equation for the plate was developed and consequently the equations of compatibility were designed to obtain the relations between the deflection and shear deformation rotation along the direction of x and y coordinates. To obtain the governing equation, this total potential energy functional was differentiated with respect to deflection. The functions for these slopes were obtained from out of plane function using the solution of compatibility equations while the solution of the governing equation is the function for the out of plane displacement. The potential energy equation was minimized with respect to coefficients of deflection after incorporating the rotations and out of plane displacement equation to generate the expression for the calculation of the critical buckling load and other functions. The stiffness properties and aspect ratios were varied to ascertain the buckling behaviour of the plate. The outcome of the numerical analysis revealed that increase in the span- thickness ratio led to increased value of the critical buckling load which implies that the plate structure is safe when the plate thickness is increased. The results obtained in this study were compared with similar works by other researchers available in the literature and were found to follow identical pattern but quite distinct in validation.

Keywords: CCCS plate, stability analysis, three-dimensional (3D) plate theory, polynomial displacement function.

Date of Submission: 05-02-2022

Date of Acceptance: 18-02-2022

I. Introduction

The captivating properties; light weight, economy, and ability to withstand loads, etc. of plate materials have made them to be widely used in different engineering field [1, 2]. Plate structures are used in structural engineering, mechanical engineering, and aerospace engineering etc., in making retaining walls, floor slabs, bridges, railways, ships etc. [3 - 4]. Plate has been grouped based on thickness as: thick, moderately thick and thin plates [5], and also based on their material properties and deformation nature as: orthotropic, isotropic, anisotropic plates, etc., based on shape as: triangular, rectangular, circular plates etc. [6 -7].

It is generally known that transverse compressive loads are the main loads which plates are usually subjected and they mainly act on the plates' mid plane. The in - plane compressive loads are forces which can be uniformly distributed over the plate's depth and applied at the edge parallel to the plate's middle plane [8]. The author in [9] stated that in - plane compressive loads can either be applied uniformly or non - uniformly on the plate boundaries, uniaxial or biaxial. The equilibrium of plates can be affected when subjected to the in - plane compressive forces. The plate can be in stable equilibrium if the in-plane compressive forces are small but if a little additional force leads to a large response - which causes the plate to be unstable, then result to buckling [10]. Buckling can either be elastic or inelastic - where elastic buckling occurs when the elastic limit of the material is greater than the critical buckling load. Plate fails when huge deflection and bending stresses occur due to the application of in - plane compressive load beyond the critical values - as such, it is vital to study and analyze the stability of plates in order to obviate failure [11 - 12].

The analysis of plates has been of paramount importance to many researchers [13, 14, 15], and different theories and methods have been deployed for this purpose by different researchers. The generally well known classical plate theory (CPT) developed by the author in [14] can be applied in the buckling analysis of thin plates only due to the non-inclusion of shear deformation which is dominant in thick plate. The CPT over-

estimates the critical buckling loads when used in the analysis of thick plate [15]. The gap in CPT in the analysis of thick plates was bridged by the formulation of refined plate theories (RPT) [16 - 17]. The RPT is a shear deformation theory which is based on the assumption that the vertical line which is normal to the mid- surface before deformation do not remain normal after deformation, but remain straight [18]. The RPT: first order shear deformation theory (FSDT) has shear correction factor as its limitation [19 - 20]. The higher order shear deformation theories (HSDT) which is an improvement on the FSDT, due to its avoidance of shear correction factor has been used by different researchers in the analysis of thick plates [21 - 24].

The results of the buckling analysis of thick plates using shear deformation theories from previous scholars proved that 2-D or incomplete 3-D analysis results for thick plates with very high depth to length ratio is unreliable [2, 25, 26]. This is because a thick plate is a 3-D member, as such, should be analyzed as such for a better result to be achieved by putting all the directions (x, y, and z) into consideration which amount into analysis having the whole six stresses and strain elements in the mathematical relations. Thus, the FSDT and the HSDT are regarded as an incomplete 3-D analysis of thick plates, as such, for complete thick plate analysis, 3-D plate theory that considers the three directions needs to be employed [25 - 27]. However, no much study has been carried out by researchers, by considering the 3-D member for stability analysis of thick plates with a view to obtaining the critical buckling loads by using the exact displacement function derived from compatibility equations.

In [25 - 27], the authors did a study on the 3-D elasticity buckling solution for rectangular thick plate that was simply supported with the use of displacement potential method. They obtained analytical solution from the method they applied for linear elastic buckling for the rectangular thick plate with simply supported edges. But they [25] an assumed the displacement function which may not be reliable, and also only considered thick rectangular plate whose edges were simply supported without applying polynomial shear deformation plate theory. They did not consider a three edge clamped and simply supported rectangular plate boundary conditions.

The author in [26] studied the application of new trigonometry shear deformation plate theory in the buckling solution of 3-D rectangular isotropic thick plate which is clamped at one edge and the other remaining edge simply supported (CSSS) under uniaxial compression using the variational method. They carried out the 3-D analysis for the plate's critical buckling by varying stiffness properties and the aspect ratio. Though the method they applied bridged the limitation of author in [25] by formulating their displacement function from the compatibility equation obtained, it can be seen in their analysis that they did not apply polynomial function which is easier to apply especially in the case of complex support conditions. They [25 - 27] only considered CSSS rectangular plate, they did not study for other boundary conditions.

The author in [28] applied trigonometric displacement function in 3-D bending analysis of thick rectangular plate by considering exact solution assumption in the analytic process. They obtain the displacements and stresses that are induced due to the applied load, but did not consider the buckling load which check the stability of the plate when subjected to an inplane loading. More so, they did not apply polynomial function which is easier to apply especially in the case of complex support conditions such as CCCS plate.

This study is aimed at bridging the gap in the literature adopting an analytical approach to obtain a close form solution for a 3-D stability analysis of an isotropic thick rectangular plate subjected to a uniform distributed inplane loading. This work aimed at establishing a more viable formula for computing the critical buckling load of thick rectangular plate which is clamped at the three edge and the other remaining edge simply supported using the 3-D polynomial function modelling technique. This model can be trustworthy in the analysis of any category of rectangular plate to obtain the exact deflection and buckling load that may occur due to applied uniaxial compressive load on the plate structure.

II. Formulation of Total Potential Energy

The research methodology of the study includes formulation of energy equation, compatibility and governing equation of thick plate under pure buckling considering an axially loaded rectangular plate as presented in figure 1.

The non-dimensional total potential energy $[\Pi]$ expression for an elastic three-dimensional plate theory of R and Q coordinates at the span-thickness aspect ratio is in line with author in [26] and presented as:

$$\begin{aligned} \Pi = D \frac{(1-\mu)ab}{2a^2(1-2\mu)} \int_0^1 \int_0^1 & \left[(1-\mu) \left(\frac{\partial \theta_{sx}}{\partial R} \right)^2 + \frac{1}{\beta} \frac{\partial \theta_{sx}}{\partial R} \cdot \frac{\partial \theta_{sy}}{\partial Q} + \frac{(1-\mu)}{\beta^2} \left(\frac{\partial \theta_{sy}}{\partial Q} \right)^2 + \frac{(1-2\mu)}{2\beta^2} \left(\frac{\partial \theta_{sx}}{\partial Q} \right)^2 \right. \\ & + \frac{(1-2\mu)}{2} \left(\frac{\partial \theta_{sy}}{\partial R} \right)^2 \\ & + \frac{6(1-2\mu)}{t^2} \left(a^2 \theta_{sx}^2 + a^2 \theta_{sy}^2 + \left(\frac{\partial w}{\partial R} \right)^2 + \frac{1}{\beta^2} \left(\frac{\partial w}{\partial Q} \right)^2 + 2a \cdot \theta_{sx} \frac{\partial w}{\partial R} + \frac{2a \cdot \theta_{sy}}{\beta} \frac{\partial w}{\partial Q} \right) \\ & \left. + \frac{(1-\mu)a^2}{t^4} \left(\frac{\partial w}{\partial S} \right)^2 - \frac{N_x}{D^*} \cdot \left(\frac{\partial w}{\partial R} \right)^2 \right] \partial R \partial Q \end{aligned} \quad (1)$$

Where:

$$D^* = D \frac{(1-\mu)}{(1-2\mu)}$$

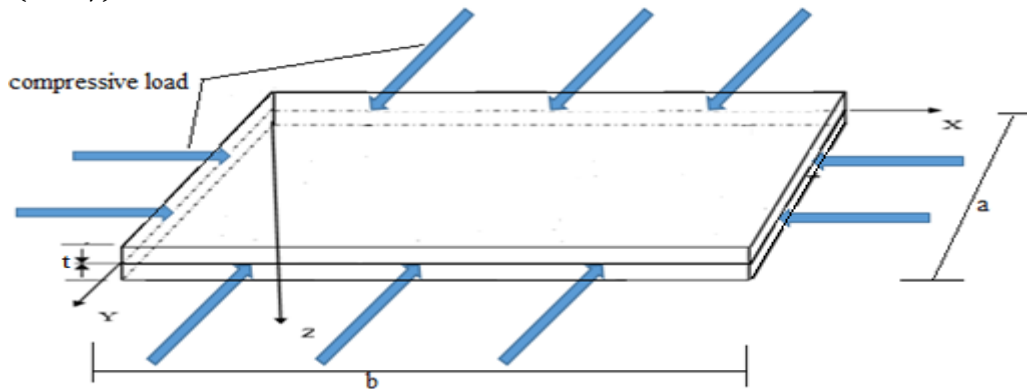


Figure 1: An axially loaded thick rectangular plate under compression

2.2. Compatibility Equation

The true compatibility equations in x-z plane y-z plane according the author in [27] is obtained by minimizing the energy equation with respect to rotation in x-z plane and rotation in y-z plane and equate its integrands to zero to get:

$$(1-\mu) \frac{\partial^2 \theta_{sx}}{\partial R^2} + \frac{1}{2\beta} \cdot \frac{\partial^2 \theta_{sy}}{\partial R \partial Q} + \frac{(1-2\mu)}{2\beta^2} \frac{\partial^2 \theta_{sx}}{\partial Q^2} + \frac{6(1-2\mu)}{t^2} \left(a^2 \theta_{sx} + a \cdot \frac{\partial w}{\partial R} \right) = 0 \quad (2)$$

$$\frac{1}{2\beta} \cdot \frac{\partial^2 \theta_{sx}}{\partial R \partial Q} + \frac{(1-\mu)}{\beta^2} \frac{\partial^2 \theta_{sy}}{\partial Q^2} + \frac{(1-2\mu)}{2} \frac{\partial^2 \theta_{sy}}{\partial R^2} + \frac{6(1-2\mu)}{t^2} \left(a^2 \theta_{sy} + \frac{a \cdot \partial w}{\beta \partial Q} \right) = 0 \quad (3)$$

Using law of addition, the Equations 2 and 3 will be simplified, then factorizing the outcome gives:

$$\frac{\partial w}{\partial R} \left[(1-\mu) \frac{\partial^2}{\partial R^2} + \frac{1}{\beta^2} \cdot \frac{\partial^2}{\partial Q^2} (1-\mu) + \frac{6(1-2\mu)a^2}{t^2} \cdot \left(1 + \frac{1}{c} \right) \right] = 0 \quad (4)$$

$$\frac{1}{\beta} \cdot \frac{\partial w}{\partial Q} \left[\frac{\partial^2}{\partial R^2} (1-\mu) + \frac{(1-\mu)}{\beta^2} \frac{\partial^2}{\partial Q^2} + \frac{6(1-2\mu)a^2}{t^2} \cdot \left(1 + \frac{1}{c} \right) \right] = 0 \quad (5)$$

After simplification using law of addition, one of the possible of Equation becomes:

$$\frac{6(1-2\mu)(1+c)}{t^2} = - \frac{c(1-\mu)}{a^2} \left(\frac{\partial^2}{\partial R^2} + \frac{1}{\beta^2} \frac{\partial^2}{\partial Q^2} \right) \quad (6)$$

2.3. General Governing Equation

The minimization of energy equation with respect to deflection gives the general governing equation as presented in [28]:

$$\frac{D^*}{2a^2} \int_0^1 \int_0^1 \left[\frac{6(1-2\mu)(1+c)}{t^2} \left(\frac{\partial^2 w}{\partial R^2} + \frac{1}{\beta^2} \frac{\partial^2 w}{\partial Q^2} \right) + \frac{(1-\mu)a^2}{t^4} \frac{\partial^2 w}{\partial S^2} - \frac{N_x}{D^*} \cdot \frac{\partial^2 w}{\partial R^2} \right] \partial R \partial Q = 0 \quad (7)$$

Substituting Equation 6 into Equation 7 and simplifying the outcome gives two governing differential equations of a 3-D rectangular plate subject to pure buckling as presented in Equation 8 and 9:

$$\frac{\partial^4 w_1}{\partial R^4} + \frac{2}{\beta^2} \cdot \frac{\partial^4 w_1}{\partial R^2 \partial Q^2} + \frac{1}{\beta^4} \cdot \frac{\partial^4 w_1}{\partial Q^4} - \frac{N_{x1} a^4}{g D^*} \cdot \frac{\partial^2 w_1}{\partial R^2} = 0 \quad (8)$$

$$\frac{(1-\mu)a^4}{t^4} \cdot \frac{\partial^2 w_s}{\partial S^2} - \frac{N_{xs} a^4}{D^*} \cdot \frac{\partial^2 w_s}{\partial R^2} = 0 \quad (9)$$

Thus, polynomial expression for deflection derived from Equation (8) is given in Equation (10) respectively as:

$$w = \Delta_0 (a_0 + a_1R + a_2R^2 + a_3R^3 + a_4R^4) \times (b_0 + b_1Q + b_2Q^2 + b_3Q^3 + b_4Q^4) \quad (10)$$

Equation (10a) and (10b) can be re-written as:

$$w = A_1 h \quad (11)$$

Where:

$$A_1 = \Delta_0 \begin{bmatrix} a_0 \\ a_1 \\ a_2 \\ a_3 \\ a_4 \end{bmatrix} \cdot \begin{bmatrix} b_0 \\ b_1 \\ b_2 \\ b_3 \\ b_4 \end{bmatrix} \quad (12)$$

$$h = [1 \ R \ R^2 \ R^3 \ R^4] \cdot [1 \ Q \ Q^2 \ Q^3 \ Q^4] \quad (13)$$

$$\theta_{sx} = \frac{A_2}{a} \cdot \frac{\partial h}{\partial R} \quad (14)$$

$$\theta_{sy} = \frac{A_3}{a\beta} \cdot \frac{\partial h}{\partial Q} \quad (15)$$

Given that: A_1 is the coefficient of deflection A_2 and A_3 are the coefficients of shear deformation in x axis and y axis respectively.

2.4. Direct Governing Equation

Direct governing equation was obtained by substituting Equations (11), (14) and (15) into Equation (1), the Energy equation becomes:

$$\begin{aligned} \Pi = \frac{D^* ab}{2a^4} & \left[(1 - \mu) A_2^2 \int_0^1 \int_0^1 \left(\frac{\partial^2 h}{\partial R^2} \right)^2 dRdQ + \frac{1}{\beta^2} \left[A_2 \cdot A_3 + \frac{(1 - 2\mu) A_2^2}{2} + \frac{(1 - 2\mu) A_3^2}{2} \right] \int_0^1 \int_0^1 \left(\frac{\partial^2 h}{\partial R \partial Q} \right)^2 \right. \\ & + \frac{(1 - \mu) A_3^2}{\beta^4} \int_0^1 \int_0^1 \left(\frac{\partial^2 h}{\partial Q^2} \right)^2 dRdQ \\ & + 6(1 - 2\mu) \left(\frac{a}{t} \right)^2 \left([A_2^2 + A_1^2 + 2A_1 A_2] \cdot \int_0^1 \int_0^1 \left(\frac{\partial h}{\partial R} \right)^2 dRdQ \right. \\ & \left. \left. + \frac{1}{\beta^2} \cdot [A_3^2 + A_1^2 + 2A_1 A_3] \cdot \int_0^1 \int_0^1 \left(\frac{\partial h}{\partial Q} \right)^2 dRdQ \right) - \frac{N_x a^2 A_1^2}{D^*} \cdot \int_0^1 \int_0^1 \left(\frac{\partial h}{\partial R} \right)^2 dRdQ \right] \quad (16) \end{aligned}$$

Differentiating Equation (16) with respect to shear deformation coefficient (A_2 and A_3), and solve simultaneously gives:

$$A_2 = \left(\frac{k_{12} k_{23} - k_{13} k_{22}}{k_{12} k_{12} - k_{11} k_{22}} \right) \cdot A_1 \quad (17)$$

$$A_3 = \left(\frac{k_{12} k_{13} - k_{11} k_{23}}{k_{12} k_{12} - k_{11} k_{22}} \right) \cdot A_1 \quad (18)$$

Let:

$$k_{11} = (1 - \mu) k_{RR} + \frac{1}{2\beta^2} (1 - 2\mu) k_{RQ} + 6(1 - 2\mu) \left(\frac{a}{t} \right)^2 k_R \quad (19)$$

$$k_{21} = k_{12} = \frac{1}{2\beta^2} k_{RQ}; \quad k_{13} = -6(1 - 2\mu) \left(\frac{a}{t} \right)^2 k_R; \quad k_{32} = k_{23} = -\frac{6}{\beta^2} (1 - 2\mu) \left(\frac{a}{t} \right)^2 k_Q \quad (20)$$

$$k_{22} = \frac{(1 - \mu)}{\beta^4} k_{QQ} + \frac{1}{2\beta^2} (1 - 2\mu) k_{RQ} + \frac{6}{\beta^2} (1 - 2\mu) \left(\frac{a}{t} \right)^2 k_Q \quad (21)$$

Where:

$$k_{RR} = \int_0^1 \int_0^1 \left(\frac{\partial^2 h}{\partial R^2} \right)^2 dRdQ \quad (22)$$

$$k_{RQ} = \int_0^1 \int_0^1 \left(\frac{\partial^2 h}{\partial R \partial Q} \right)^2 dRdQ \quad (23)$$

$$k_{QQ} = \int_0^1 \int_0^1 \left(\frac{\partial^2 h}{\partial Q^2} \right)^2 dRdQ \quad (24)$$

$$k_R = \int_0^1 \int_0^1 \left(\frac{\partial h}{\partial R}\right)^2 dRdQ \tag{25}$$

$$k_Q = \int_0^1 \int_0^1 \left(\frac{\partial h}{\partial Q}\right)^2 dRdQ \tag{26}$$

Differentiating Equation (16) with respect to deflection coefficient (A_1) and simplifying the outcome, an expression for the critical buckling load (N_{xcr}) is established as:

$$\frac{N_{xa}^2}{D^*} = 6(1 - 2\mu) \left(\frac{a}{t}\right)^2 \left[\left[1 + \left(\frac{k_{12}k_{23} - k_{13}k_{22}}{k_{12}k_{12} - k_{11}k_{22}}\right) \right] + \frac{1}{\beta^2} \cdot \left[1 + \left(\frac{k_{12}k_{13} - k_{11}k_{23}}{k_{12}k_{12} - k_{11}k_{22}}\right) \right] \cdot \frac{k_Q}{k_R} \right] \tag{27}$$

Similarly:

$$N_{xcr} = \frac{(1 + \mu)Et^3}{2a^2} \left(\frac{a}{t}\right)^2 \left[\left[1 + \left(\frac{k_{12}k_{23} - k_{13}k_{22}}{k_{12}k_{12} - k_{11}k_{22}}\right) \right] + \frac{1}{\beta^2} \cdot \left[1 + \left(\frac{k_{12}k_{13} - k_{11}k_{23}}{k_{12}k_{12} - k_{11}k_{22}}\right) \right] \cdot \frac{k_Q}{k_R} \right] \tag{28}$$

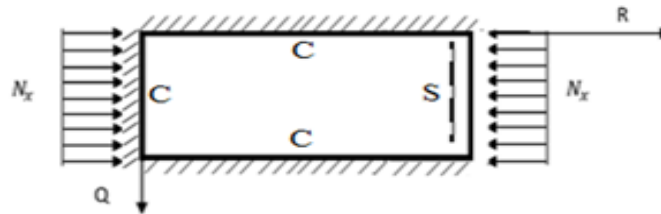


Figure2: CCCS rectangular plate

Table 1: Polynomial Stiffness coefficient values of CCCS plate

TYPE	PLATE	k_{RR}	k_{RQ}	k_{QQ}	k_R	k_Q	k_q
Polynomial	CCCS	0.0028571	0.0016327	0.0060317	0.0001361	0.00014361	0.0025

III. Results and Discussions

In this section, a numerical analysis of the critical buckling load of the three-dimensional plate at varying stiffness and aspect ratio ($\beta = b/a$) are presented considering the equation obtained in the previous section. In the result presentation, the aspect ratio which is the ratio of the length and breadth of the plate is varied between 1.0, 1.2, 1.3, 1.4, 1.5, 1.6, 1.7, 1.8 and 2.0 with respect to the plates thickness. Similarly, the span to thickness ratio of the plate is varied between 4, 7, 10, 15 20, 30, 40, 50, 60, 70, 80, 90, 100, 1000 and 1500 with respect to the width of the plate.

The Table 2 contains the result of non-dimensional critical buckling load on the CCCS rectangular plate using polynomial function at varying aspect ratio. The result shows that the non-dimensional value of critical buckling load (N_{xcr}) increases as the aspect ratio of the plate decreases. This might indicate that the chance of failure in a plate structure increases with an increase in plate breadth of the plate. Similarly, the results obtained in Table 2 pointed out that the values of critical buckling load increase as the span- thickness ratio increases. This reveals that the failure in a plate structure is bound to occur as the in-plane load on the plate increases and gets to the critical buckling. This implies that reducing the thickness of the plate increases the tendency of failure in a plate structure. To overcome this, higher thickness or increased thickness with respect to the span of the plate is advised.

From Table 2 and Figure 3, 4, 5, 6 presented here, it is observed that as the in-plane load which will cause the plate to fail by compression increases from zero to critical buckling load (N_{xcr}), the buckling of the plate exceeds specified elastic limit thereby causing failure in the plate structure. This means that, the load that causes the plate to deform also causes the plate material to buckle simultaneously.

In validation of the result of the present study, a comparative analysis is performed to show the degree of divergence between the result of the present study with those of classical plate theory (CPT), and refined plate theory (RPT) as presented in Table 3, it was discovered that as the span-thickness ratio increases, the results of the present study become closer to those obtained using the CPT [30, 31] and closest to those using RPT [32] at aspect ratio between 1.0 and 1.4. This value begins to vary as the aspect ratio increases (beyond 1.5). This is quite expected because increase in the plates aspect ratio decreases the capacity of plate to resist buckling. Moreover, the result of the result of percentage difference being lower is quite expected because RPT predict more close-form solution and are economical in use compared to the CPT. However, it can be said that the values obtained are in agreement with those obtained in the literature. It is noticed that the present theory converges faster with RPT than the CPT. This confirms the accuracy of the derived relationships and proved the reliability of the present model for thick plate analysis.

The credibility of the relationship is given in the percentage difference calculation as in the Table 3 and Figure 7. The average percentage difference between the present study (at $a/t = 7$) and those of Ibearugbulem *et al.* [30], Ventsel & Krauthammer [31] and Uzoukwu *et al.* [32] is about 4.67%, 4.70% and 4.77% respectively. Meanwhile, the overall percentage difference the present work and all the three previous studies in comparison is about 4.7%. This means that at about 95% confidence level, the values from the present study are the same with those from past scholars.

The comparative analysis performed reveal that, the present three-dimensional plate theory agreed well with other theories (CPT and RPT), though showed more level of accuracy and can be used effectively for stability analysis of any category of plate ranging from thin (CPT), moderately thick (RPT) and thick (3D) plate to find the condition of plate where failure occurs with or without application of load by getting the exact load that induce buckling in the plate structure.

Table 2: Non-dimensional critical buckling load (N_{xcr}) on the CCCS rectangular plate using polynomial function

$\alpha = \frac{a}{t}$	$N_{xcr} = \frac{N_x D}{a^2}$								
	$\beta = 1.0$	$\beta = 1.2$	$\beta = 1.3$	$\beta = 1.4$	$\beta = 1.5$	$\beta = 1.6$	$\beta = 1.7$	$\beta = 1.8$	$\beta = 2.0$
4	60.04453	44.2948	39.4294	35.7621	32.9449	30.7437	28.9973	27.5924	25.5054
7	86.09212	59.8990	52.2807	46.7061	42.5289	39.3322	36.8400	34.8646	31.9798
10	96.56504	65.6462	56.8782	50.5361	45.8276	42.2515	39.4805	37.2951	34.1220
15	103.3038	69.1973	59.6830	52.8508	47.8075	43.9946	41.0510	38.7366	35.3873
20	105.8966	70.5341	60.7318	53.7121	48.5416	44.6391	41.6306	39.2677	35.8527
30	107.8319	71.5216	61.5041	54.3448	49.0799	45.1112	42.0548	39.6562	36.1926
40	108.5266	71.8739	61.7791	54.5699	49.2711	45.2788	42.2053	39.7939	36.3131
50	108.8512	72.0381	61.9072	54.6746	49.3602	45.3568	42.2753	39.8580	36.3692
60	109.0284	72.1276	61.9770	54.7317	49.4087	45.3993	42.3134	39.8929	36.3997
70	109.1355	72.1818	62.0192	54.7662	49.4380	45.4250	42.3365	39.9140	36.4181
80	109.2052	72.2169	62.0466	54.7886	49.4570	45.4416	42.3514	39.9277	36.4301
90	109.2530	72.2411	62.0654	54.8040	49.4700	45.4531	42.3617	39.9371	36.4383
100	109.2872	72.2583	62.0789	54.8150	49.4794	45.4613	42.3690	39.9438	36.4442
1000	109.4319	72.3313	62.1357	54.8614	49.5188	45.4958	42.4001	39.9722	36.4690
1500	109.4327	72.3317	62.1361	54.8616	49.5191	45.4960	42.4002	39.9724	36.4692

From Figure 5, 6 and Tables 3 and 4, the present study showed good agreement with previous studies but varied widely when considered as thick plate at span to thickness ratios of 4 and 7. The total average percentage difference between the present study compared with previous studies is 4.7% at span to thickness ratio of 7. This value which is less than 5% is sufficient in the statistical analysis showed that the present method can be used with confidence for buckling analysis of CCCS thick plate.

IV. Conclusion ad Recommendation

From the result obtained in this study, it is observed that CPT and gives reliable results in thin plates, but over-predicts buckling loads in relatively thick plates. Also, the RPT gives is an approximate relation for buckling analysis of thick plate, whereas 3-D theory yields an exact solution. This proved that the displacement functions (polynomial and trigonometric) developed in this work are recommended for the thick plate analysis.

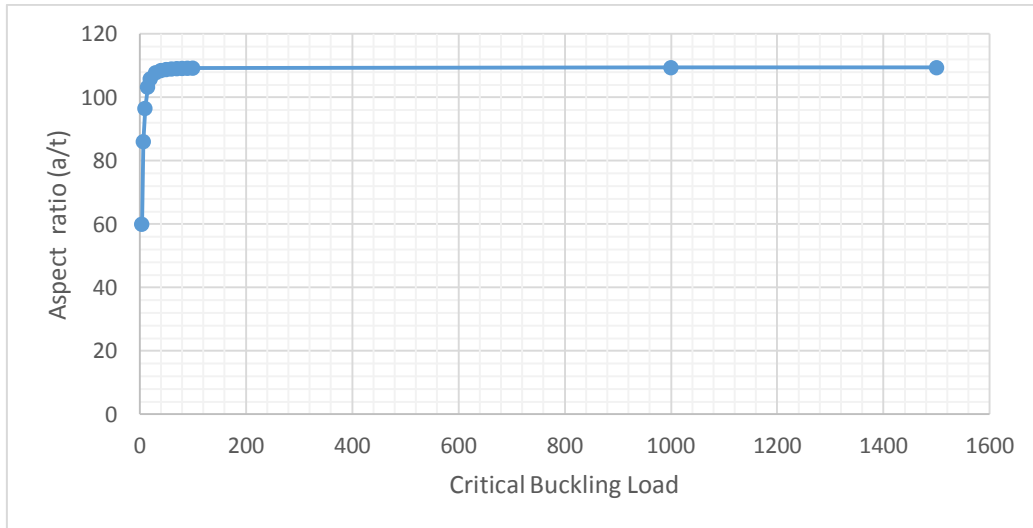


Figure 3: Graph of Critical buckling load ($N_{xcr} = \frac{N_x D}{a^2}$) versus aspect ratio of a square rectangular plate.

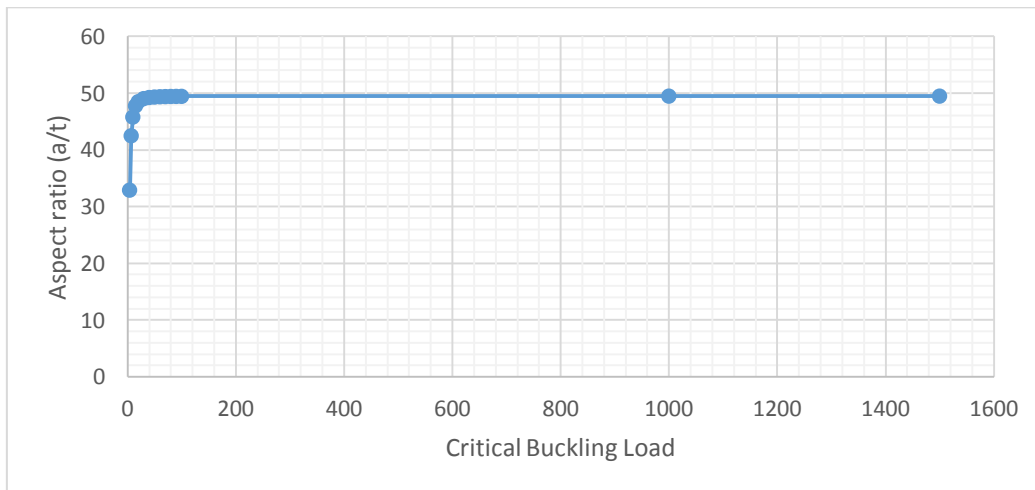


Figure 4: Graph of Critical buckling load ($N_{xcr} = \frac{N_x D}{a^2}$) versus aspect ratio of a rectangular plate at length-width ratio of 1.5

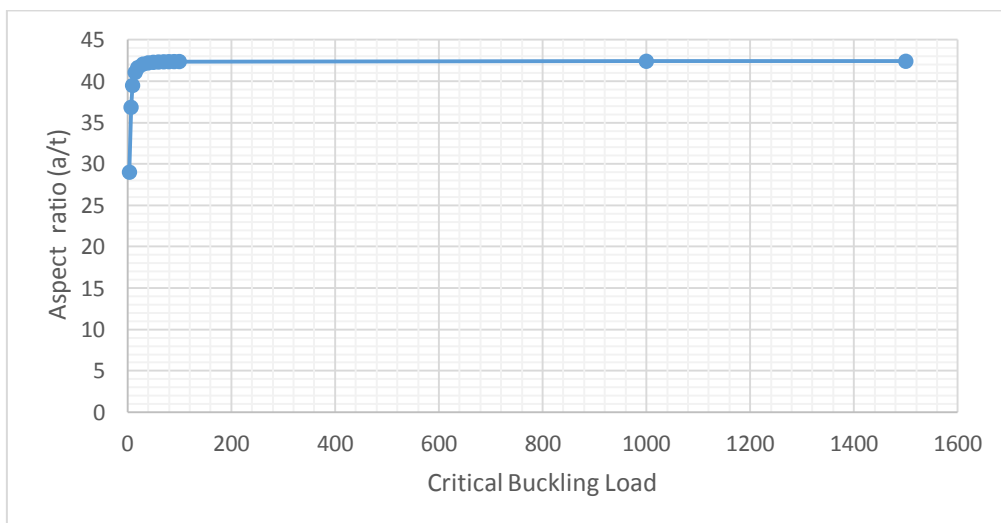


Figure 5: Graph of Critical buckling load ($N_{xcr} = \frac{N_x D}{a^2}$) versus aspect ratio of a rectangular plate at length-width ratio of 1.7

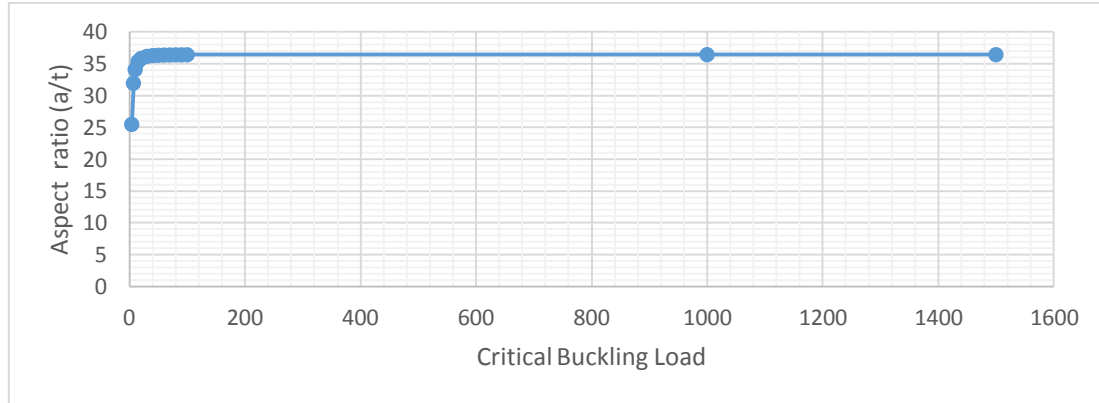


Figure 6: Graph of Critical buckling load ($N_{xcr} = \frac{N_x D}{a^2}$) versus aspect ratio of a rectangular plate at length-width ratio of 2.0

Table 3: Results of the Present Study Compared with the Results of previous studies on CCCS Plate for a/t=7

Aspect ratio P=b/a	Critical Buckling Load Coefficients				% Difference b/w [29] & [P.S]	% Difference b/w [30] & [P.S]	% Difference b/w [31] & [P.S]
	Ibearugbulem <i>et al</i> [30]	Ventsel & Krauthermmer [31]	Uzoukwu <i>et al</i> , [32]	Present Study [P.S]			
1.0	89.3539	89.3372	89.2269	86.0921	3.7887	3.7693	3.6412
1.2	59.0597	59.0463	58.9756	59.8990	1.4012	1.4236	1.5416
1.3	50.7347	50.7218	50.6625	52.2807	2.9571	2.9818	3.0952
1.4	44.7949	44.7769	44.7313	46.7061	4.0920	4.1305	4.2281
1.5	40.4325	40.4154	40.3753	42.5289	4.9294	4.9696	5.0639
1.6	37.1476	37.1315	37.0952	39.3322	5.5542	5.5952	5.6875
1.7	34.6198	34.6048	34.5711	36.8400	6.0266	6.0673	6.1588
1.8	32.6373	32.6225	32.5917	34.8646	6.3884	6.4309	6.5192
2.0	29.7769	29.7638	29.7356	31.9798	6.8884	6.9294	7.0176
Average Percentage Difference					4.67	4.70	4.71

Total Average Percentage Difference = 4.71

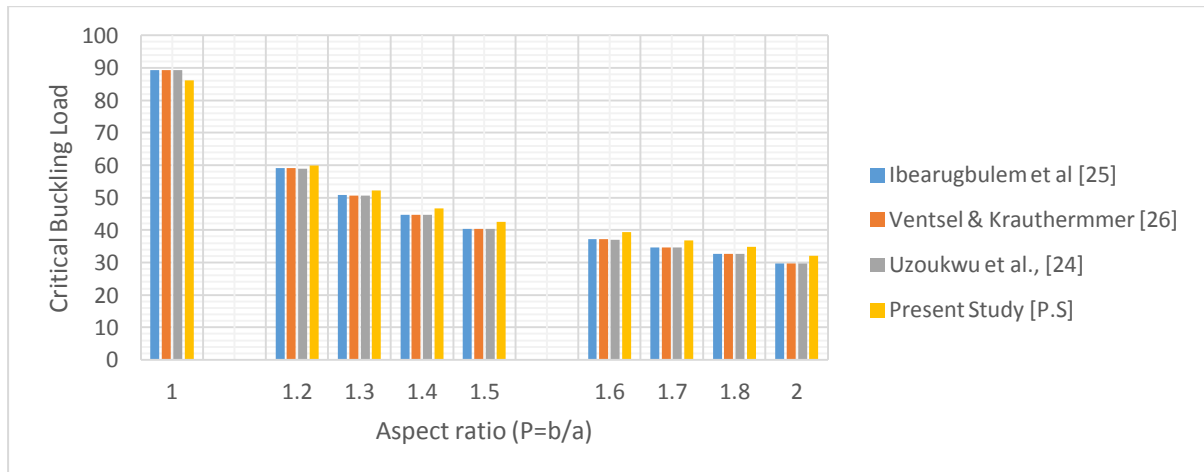


Figure 7: Graph of critical buckling load against aspect ratio (b/a) on comparative analysis of results from previous and present study at span-thickness ratio of 7

Reference

- [1]. Ibearugbulem, O. M, Onyeka, F. C. (2020). Moment and Stress Analysis Solutions of Clamped Rectangular Thick Plate. *EJERS, European Journal of Engineering Research and Science*, 5(4): 531-534. DOI: <http://dx.doi.org/10.24018/ejers.2020.5.4.1898>.
- [2]. Onyeka, F. C. (2020). Critical lateral load analysis of rectangular plate considering shear deformation effect. *Global Journal of Civil Engineering*, Vol. 1: 16–27. doi:10.37516/global.j.civ.eng.2020.0121.
- [3]. Ghugal, Y. M., Gajbhiye, P.D. (2016). Bending analysis of thick isotropic plates by using 5th order shear deformation theory. *Journal of Applied and Computational Mechanics*, Vol. 2(2): 80-95.
- [4]. Onyeka, F. C., Osegbowa, D.E. (2020). Stress analysis of thick rectangular plate using higher order polynomial shear deformation theory. *Futo Journal Series (FUTOJNLS)*, Vol. 6(2): 142-161
- [5]. Chandrashekhara, K. (2000). *Theory of plates*. University Press (India) Limited.
- [6]. Nwoji C.U., Mama B.O., Onah H.N., Ike C.C. (2017). Kantorovich-Vlasov method for simply supported rectangular plates under uniformly distributed transverse loads. *International Journal of Civil, Mechanical and Energy Science (IJCMES)*, Vol. 3(2): 69-77.

- [7]. Onyeka, F.C., Osegbowa, D., Arinze, E.E. (2020). Application of a new refined shear deformation theory for the analysis of thick rectangular plates. *Nigerian Research Journal of Engineering and Environmental Sciences*, Vol. 5(2): 901-917.
- [8]. Timoshenko, S., Gere, J.M. (1963). *Theory of elastic stability*, 2nd Edition. McGraw-Hill Books Company, New York,
- [9]. Michael, E.O, Eghosa, O.R., Charles C.I. (2020). Elastic buckling analysis of SSCF and SSSS rectangular thin plates using the single finite Fourier sine integral transform method. *International Journal of Engineering Research and Technology*, Vol. 13(6): 1147-1158.
- [10]. Sayyada, A. S., Ghugal, Y.M. (2012) Buckling analysis of thick isotropic plates by using exponential Shear deformation theory. *Applied and Computational Mechanics*, Vol. 6: 185 – 196.
- [11]. Wang, C.M, Wang, C.Y., Reddy, J.N. (2005). *Exact solutions for buckling of structural members*. Boca Raton Florida, CRC Press LLC.
- [12]. Sachin, M.G, Rajesh, B.H, Atteshamuddin, S.S, Manas D.G. (2015). Buckling analysis of thick plates using refined trigonometric shear deformation theory. *Journal of Materials and Engineering Structures*, Vol. 2: 159-167.
- [13]. Ibearugbulem, O.M., Ebirim, S.I., Anya, U.C., Ettu, L.O. (2020). Application of Alternative II theory to vibration and stability analysis of thick rectangular plates (isotropic and orthotropic). *Nigerian Journal of Technology (NIJOTECH)*, Vol. 39(1): 52-62. <http://dx.doi.org/10.4314/njt.v39i1.6>
- [14]. Kirchhoff, G.R. (1850). U'ber das Gleichgewicht and die Bewegung einer elastschen Scheibe. *Journal f' ur die reine und angewandte Mathematik*, Vol. 40: 51-88 (in German).
- [15]. Sayyad, A.S., Ghugal, Y.M. (2012). Buckling analysis of thick isotropic plates by using exponential shear deformation theory. *Applied and Computational Mechanics*, Vol. 6: 185-196.
- [16]. Ibearugbulem, O.M., Ezech, J.C., Ettu, L.O. (2014). *Energy methods in theory of rectangular plates (use of polynomial shape functions)*. Liu House of Excellence Ventures, Owerri: 10 – 20.
- [17]. Ibearugbulem, O. M., Njoku, K.O., Eziefula, U.G. (2016). *Full shear deformation for analysis of thick plate*. Proceedings of Academics World 43rd International Conference, Rome, Italy.
- [18]. Reissner, E. (1945). The effect of transverse shear deformations on the bending of elastic plates. *ASME Journal of Applied Mechanics*, Vol. 12: A69-A77.
- [19]. Mindlin. R.D. (1951). Influence of rotary inertia and shear on flexural motion of isotropic elastic plates. *ASME Journal of Applied Mechanics*, Vol. 18: 31-38.
- [20]. Yang, Z., Qian, X. (2017). Analysis bending solutions of clamped rectangular thick plate *Hindawi Mathematical Problems in Engineering*, Vol. 17: 1-6.
- [21]. Gunjal, S.M., Hajare, R.B., Sayyad, A.S., Ghodle, M.D. (2015). Buckling analysis of thick plates using refined trigonometric shear deformation theory. *Journal of Materials and Engineering Structures*, Vol. 2: 159-167.
- [22]. Ezech, J.C., Onyechere, I.C., Ibearugbulem, O.M., Anya, U.C., Anyaogu, L. (2018). Buckling analysis of thick rectangular flat SSSS plates using polynomial displacement functions. *International Journal of Scientific & Engineering Research*, Vol. 9(9): 387-392.
- [23]. Ibearugbulem, O.M., Ezech, J.C., Ettu, L.O., Gwarah, L.S. (2018). Bending analysis of rectangular thick plate using polynomial shear deformation theory. *IOSR Journal of Engineering (IOSRJEN)*, Vol. 8(9): 53-6.
- [24]. Onyeka, F.C., Okafor, F.O., Onah, H.N. (2019). Application of exact solution approach in the analysis of thick rectangular plate. *International Journal of Applied Engineering Research*, Vol. 14(8): 2043-2057.
- [25]. Vareki, A.M., Neya, B.N., Amiri, J.V., (2016). 3-D elasticity buckling solution for simply supported thick rectangular plates using displacement potential functions. *Applied Mathematical Modelling*, Vol. 40: 5717–5730.
- [26]. Onyeka, F.C., Okafor, F.O., Onah H.N. (2021). Application of a new trigonometric theory in the buckling analysis of three-dimensional thick plate. *International Journal on Emerging Technologies*, Vol. 12(1): 228-240.
- [27]. Onyeka, F.C., Okafor, F.O., Onah H.N. (2021). Buckling solution of a three-dimensional clamped rectangular thick plate using direct variational method. *IOSR Journal of Mechanical and Civil Engineering (IOSR-JMCE)*, Vol. 18(3 Ser. III): 10-22.
- [28]. Onyeka, F.C., Mama, B.O. (2021). Analytical study of bending characteristics of an elastic rectangular plate using direct variational energy approach with trigonometric function. *Emerging Science Journal*, Vol. 5(6): 916–926.
- [29]. Onyeka, F.C., Mama, B.O., Okeke, T.E. (2022). Exact three-dimensional stability analysis of plate using a direct variational energy method. *Civil Engineering Journal*, Vol. 8(1): 60–80.
- [30]. Ibearugbulem, O.M. (2014). Using the product of two mutually perpendicular truncated polynomial series as shape function for rectangular plate analysis. *International Journal of Emerging Technologies and Engineering (IJETE)*. Conference proceeding, 30th – 31st August 2014, 1- 4.
- [31]. Ventsel, E., Krauthammer, T. (2001). *Thin plates and shells: theory, analysis and applications*. New York: Marcel Dekker.
- [32]. Uzoukwu S., Ibearugbulem O.M., Okere C. E., Arimanwa J. I. (2021). Stability analysis of rectangular CCSS and CCCS isotropic plates using 3rd order energy functional. *Global Scientific Journals*. Vol. 9(1): 637-649

Onyeka, F. C, et. al. "Stability Analysis of a Three-Dimensional Rectangular Isotropic Plates With Arbitrary Clamped And Simply Supported Boundary Conditions." *IOSR Journal of Mechanical and Civil Engineering (IOSR-JMCE)*, 19(1), 2022, pp. 01-09.